*Journal of Thermal Analysis and Calorimetry, Vol. 95 (2009) 3, 977–983*

# THERMAL ANALYSIS OF SOYBEAN OIL BASED POLYOLS

*B. Lin, L. Yang*, H. Dai, Q. Hou and L. Zhang*

School of Chemistry and Environment, South China Normal University, Guangzhou P. R. China 510631

Soybean oil based polyols (5-OH polyol, 10-OH polyol and 15-OH polyol) were synthetised from epoxidized soybean oil. The melting peak of polyols and the relationship between melting peak and the number-average functionality of hydroxyl in polyols were investigated by differential scanning calorimetry (DSC). The thermal decomposition of polyols and some of their thermal properties by thermogravimetry (TG) and derivative thermogravimetry (DTG) were also studied. The thermal stability of polyols in a nitrogen atmosphere was very close hence they had a same baseplate of triglyceride for polyols. The extrapolated onset temperature of polyols in their thermal mass loss, first step had a decreasing order: 5-OH polyol>10-OH polyol>15-OH polyol due to the difficulty in forming multiple elements ring of them had the same order.

The thermal behavior of polyols under non-isothermal conditions using Friedman's differential isoconversional method with different heating rates indicated that the 5-OH polyol had the lowest activation energy in thermal decomposition amongst these polyols according to the same fractional mass loss because of the weakest intramolecular oligomerization. The 15-OH polyol was prior to reach the mass loss region because the six-member ring is more stable than the three-member ring from 10-OH polyol and more easily formed.

***Keywords:*** *Friedman's analysis, polyol, soybean oil, thermal stability, thermogravimetry*

## Introduction

Thermogravimetry as a thermoanalytical method presents many advantages as a result of its precision, sensitivity, expeditiousness, and the small sample amount required in each experimental test. In recent years, thermal analysis has been successfully used for the determination of physical properties and the study of chemical reaction [1–8]. On the other hand, the thermogravimetry technique is useful in the investigation of the thermal stability of vegetable oils and their derivatives [9, 10].

Soybean oil based polyol which is derivative of soybean oil; its thermal stability depends on its chemical structure with a high content of hydroxyl. This property is of great practical importance in avoiding the rupture of glyceryl chain of these polyols, especially when the polyol reacts with 2,4-toluene diisocyanate (TDI), 4,4'-methylenebis(phenyl isocyanate) (MDI), 1,6-hexamethylene diisocyanate (HDI) and other type of diisocyanate to produce polyurethane elastomers, foams and resins as these chemosynthesis reaction are drastic exothermic foaming reaction [11]. Soy oil based polyols of 5-OH polyol, 10-OH polyol and 15-OH polyol have some similarities in the TG and DTG curves due to the triglyceride as the same baseplate for polyols [6]. Thus, knowing the thermokinetic studies by thermogravimetry are very important in these formal polyols. The acyl groups joined with the glyceryl short carbon chains present in the acylglyceride molecule was different in these formal polyols which would affect the detailed decomposition process [6].

## Experimental

### *Materials*

The epoxidized soybean oil (ESO) used in this research was kindly supplied by Nanhai Oil Co. Ltd. with a molecular mass of 985 (ESI-MS) and with a 4.375 mol kg$^{-1}$ epoxy oxygen content. Deuterated acetone (D, 99.9%) was supplied by Cambridge Isotope Laboratories, Inc., Andover, MA, USA. Diethanolamine [$NH(CH_2CH_2OH)_2$], methanol ($CH_3OH$), sulfuric acid ($H_2SO_4$), fluoboric acid ($HBF_4$), N,N-dimethylfornamide (DMF), chloroform, isopropyl alcohol, potassium bromide (KBr) and sodium sulfate anhydrous ($Na_2SO_4$) were all analytically pure grade, and were purchased from Guangzhou Chemical Reagent Co. Ltd.

### *Synthesis of soy oil based polyols*

#### Synthesis of 5-OH polyol

The definitely mass of aforementioned ESO (40.0 g) with 0.2 mass%, the $BF_3 \cdot Et_2O$ was used as the cata-

---

[*] Author for correspondence: yanglt63@yahoo.com.cn; yanglt@scnu.edu.cn

*1388–6150/$20.00*

*Akadémiai Kiadó, Budapest, Hungary*
*Springer, Dordrecht, The Netherlands*

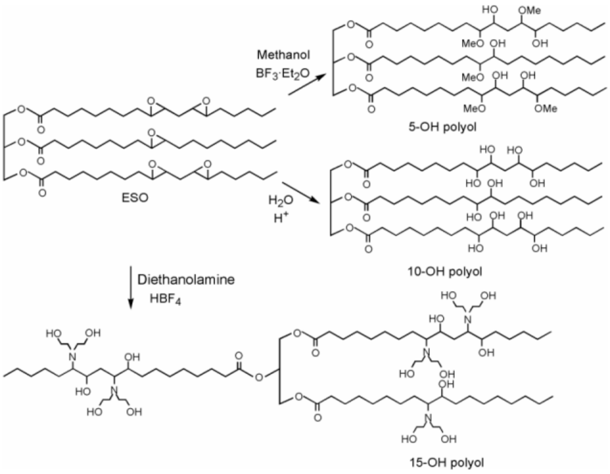

**Scheme 1** Idealized synthesis route of polyols

lyst, were both put in a four-necked reaction flask equipped with a reflux condenser and heated to the prearranged constant temperature (40±1°C) in a water bath with a mechanical stirrer for half an hour. Then 33.81 g methanol was added into the flask. Finally, the reaction mixture was heated up to 75±1°C for 6 h, at which point ammonia (30% in water, 2 mL) was added to quench the reaction. The product was washed with distilled deionised water until it was neutral to litmus and removed on a rotary evaporator with high vacuum equipment, and dried over anhydrous sodium sulfate. Finally the raw product was pressure-filtered. The product, a light-yellow viscous liquid, was isolated with a yield of 94%.

### Synthesis of 10-OH polyol

The epoxy ring of ESO, when opened up under acidic conditions, will give a formal diol from each epoxy group. In a typical procedure, ESO (26.5 g) was mixed four times its mass (104 g) of 8% sulfuric acid solution in a 250 mL three-neck round-bottomed flask, fitted with a mechanical stirrer, thermometer, and reflux condenser. The sulfuric acid solution was added dropwise for 2 h and the reaction mixture was heated under reflux for 24 h while the reaction temperature was maintained at 70±1°C. The product, extracted in chloroform, was then washed with distilled deionised water until neutral to litmus and dried over anhydrous sodium sulfate; finally the raw product was followed by pressure-filtered. The product, a pale yellow viscous liquid was isolated at 95% yield.

### Synthesis of 15-OH polyol

For preparation of the 15-OH polyol, ESO and diethanolamine were reacted together at a reflux in the presence of isopropyl alcohol at 70±1°C. In a typical procedure, ESO (25.4 g) was mixed with twice its mass of isopropyl alcohol, with 2 g $HBF_4$ as the catalyst for opening reaction of epoxy ring of ESO, and a molar excess of diethanolamine (26.4 g) in a 250 mL three-neck round-bottom flask, fitted with a mechanical stirrer, thermometer, and reflux condenser. After 28 h, the isopropyl alcohol was removed from the product in a vacuum rotary evaporator. The product was separated and washed with distilled deionised water to completely remove excess diethanolamine. The raw product was dried over anhydrous sodium sulfate then pressure-filtered. A pale yellow honey product, with an isolated yield of 90% was obtained.

In all the experiments, the components of epoxidized soybean oil and the polyols were separated in a 60–120 mesh silica gel column using a solvent system consisting of toluene and varying proportions of ethyl acetate, for spectroscopic characterization. The molecular mass (*MW*) was determined by the method of electrospray ionization-mass spectrometry (ESI-MS, WATERS, USA) analysis; the *MW* of 5-OH polyol, 10-OH polyol and 15-OH polyol were 1056, 1068 and 1439, respectively.

## *Methods*

FTIR spectra (IR Prestige-21, Shimadzu, Japan) of the prepared soybean polyols based on the oxirane cleavage by methanol, sulfuric acid and diethanolamine showed that in comparison with the spectrum of ESO, the disappearance of epoxy groups at 825, 843 $cm^{-1}$, the emergence of hydroxyl group at 3452 $cm^{-1}$, and the presence of characteristically secondary hydroxyl groups at 1098 $cm^{-1}$ can be observed in these polyols. Otherwise, the flex vibration of the C–N single bond at 1625 $cm^{-1}$ in 15-OH polyol differed distinctly from 10-OH polyol. These data illustrated the synthesis of polyols were feasible.

$^1$H-NMR spectra (Varian 400 spectrometer, USA) of the polyols and the ESO samples reveal information regarding different functional groups. The epoxy protons presents in ESO normally at 3.1 ppm is largely replaced with secondary hydroxyl group and completely disappeared in polyols.

### Characterization of thermoproperties

Melting points were obtained with a Netzsch DSC 200-PC differential scanning calorimeter (DSC) operating in $N_2$ atmosphere (20 mL $min^{-1}$). The DSC instrument was calibrated with an indium standard and Al was used as reference material. A sample of about 10 mg was scanned at a heating rate of 10°C $min^{-1}$.

The thermostability was tested by thermogravimetry (TG) and derivative thermogravimetry (DTG) with a Netzsch STA 409 PC/PG analyzer instrument in a dynamic $N_2$ atmosphere (30 mL min$^{-1}$). About 12–14 mg of sample was placed in a platinum cell which was transferred to the detector plate, and the furnace was then heated at four heating rates (5, 10, 15 and 20°C min$^{-1}$).

The raw data were converted to ASCII files and kinetic analysis was carried out using an in-house program and a Netzsch thermokinetic Program (Version 4.8.1) in the calculation procedure. The corresponding kinetic parameters were computed by non-linear regression which was the iterative calculation of the minimum sum of least squares, LSQ. For the solution of the system of differential equations, a 5$^{th}$-degree Runge–Kutta method (Prince–Dormand algorithm) was employed as a subprogram tied into a hybrid regularized Gauss–Newton method.

## Results and discussion

### *Melting points of polyols*

Physical properties of the polyols were related to the structural order and the physical state of the polyols above or below the melting point [12].

DSC curves of the prepared soy polyols differed significantly from one another and the starting material ESO (Fig. 1). All polyols displayed at one of the highest melting peaks above 3.4°C; the values are listed in Table 1. Multiple peaks in these polyols and ESO were ascribed to different crystalline polymorphs that were present in soybean oil [13]. ESO displayed a double peak at –11.3 and –5.3°C. The 5-OH polyol and 10-OH polyol were still liquid at room temperature. 5-OH polyol had one melting peak at 3.4°C and 10-OH polyol two melting peaks at –8.3 and 6.5°C. Hydrogenation caused the shift of the melting points to the higher temperatures to –5.0 and 18.9°C, giving solid grease at room temperature. However, the size of the melting peak was controlled by the crystallization rate and the physical state was largely determined by hydrogen bonding. Increasing the OH content caused an increase in viscosity and an eventual transition from liquid to grease state. The highest melting had the following order in the polyols: 5-OH polyol<10-OH polyol<15-OH polyol, due to the content of hydrogen groups in the polyols being in the same order. In a comparison of the melting peaks of polyols from 5-OH polyol to 10-OH polyol, the shape of melting peak was more and more smooth and widened. It illustrated that the introduction of more functional hydroxyl groups into the soybean oil by the oxirane cleavage reaction with $CH_3OH$, $H_2O$ and $NH(CH_2CH_2OH)_2$ caused a shift and deformation of the melting peak. Hydroxyl groups were introduced in this chemosynthesis reaction and eventually resulted in different number-average functionality of hydroxyl in the resultant polyol [12].

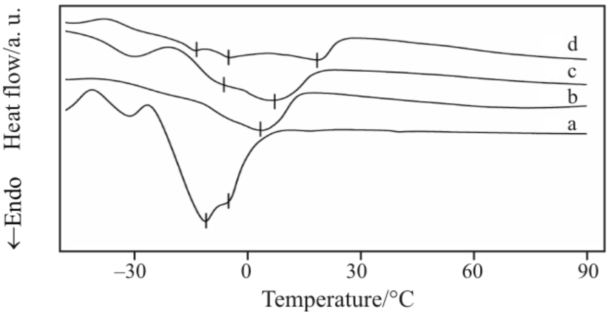

**Fig. 1** DSC curves of soy based polyols; a – ESO; b – 5-OH polyol; c – 10-OH polyol; d – 15-OH polyol

**Table 1** Melting point of ESO and polyols

| Peak | *T*/°C | | | |
|---|---|---|---|---|
| | ESO | 5-OH | 10-OH | 15-OH |
| 1 | –11.3 | 3.4 | –8.3 | –14.3 |
| 2 | –5.3 | – | 6.5 | –5.0 |
| 3 | – | – | – | 18.9 |

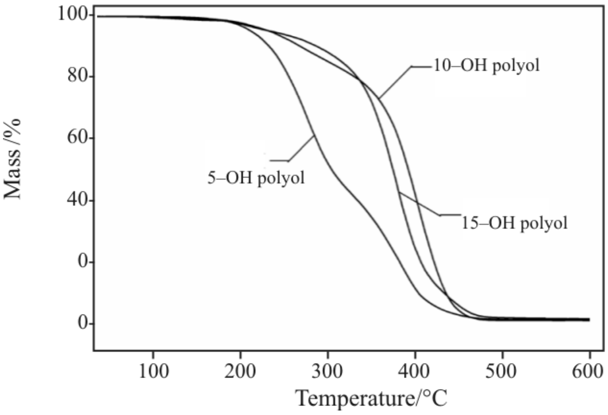

**Fig. 2** TG profiles of polyols at 10°C min$^{-1}$ under nitrogen atmosphere

### *Thermostability of polyols*

The TG profile of thermal decomposition progresses for three polyols is shown in Fig. 2 and the more detailed and more exact thermal decomposition progresses, DTG curves, are shown in Fig. 3. A summary of the TG results for the three polyols under nitrogen atmosphere is showed in Table 2. It could be seen that the stabilities are similar to each other under nitrogen atmosphere. However, the more hydroxyl in the formal polyols, the higher the stability is. This could also be explained by the higher hydroxyl equivalents of the polyols.

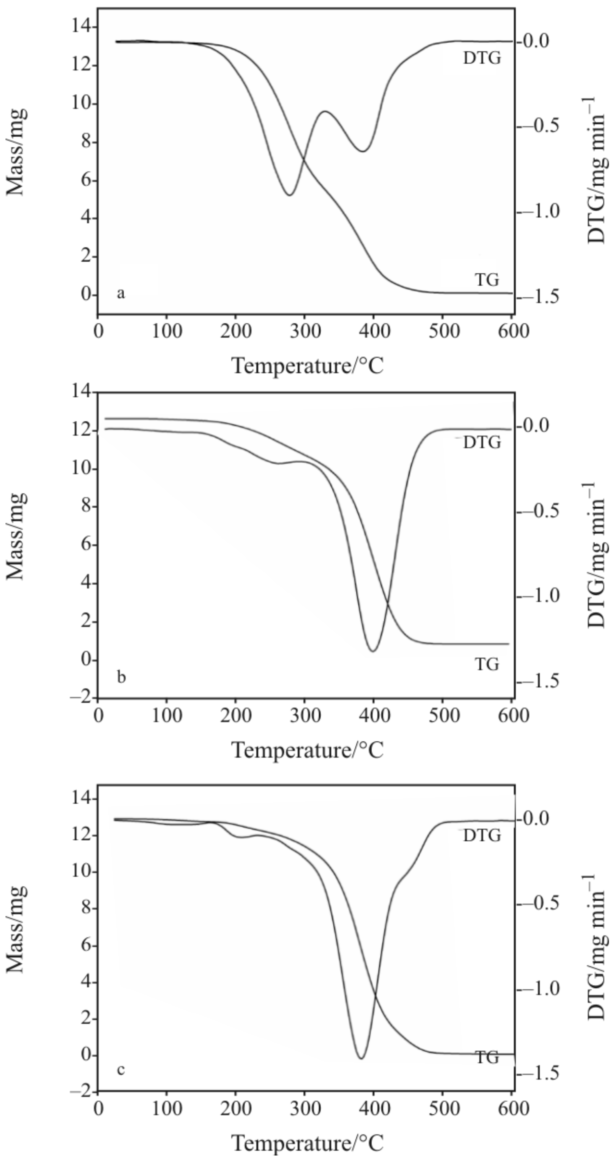

**Fig. 3** TG and DTG curves obtained using a heating rate of 10°C min$^{-1}$ under dynamic nitrogen atmosphere with a flow rate of 30 mL min$^{-1}$; a – 5-OH polyol, b – 10-OH polyol, c – 15-OH polyol

TG curves corresponding to the three studied compounds exhibit some common characteristics and the data are shown in Table 2:

- An insignificant mass loss below 150°C due to the humidity or the reaction reagent from the chemosynthesis of these polyols which is unimportant for our further discussion.
- The first mass loss step corresponds to the loss of water from hydroxyl groups and part fatty carbon chains for formal 5-OH polyol and 10-OH polyol and only water from hydroxyl for the 15-OH polyol.
- The second mass loss step corresponds to the loss of fatty carbon chains with three-membered ring for 5-OH polyol and 10-OH polyol and corresponding to the loss of fatty carbon chains with more stability six-membered ring.
- The 15-OH polyol has the third mass loss step which corresponds to the loss of higher decomposition temperature of nitride and the other ones have not this mass loss step.

At the beginning of the polyol decomposition, slight mass loss was noticed (Fig. 3), which could be the result of the remains of the reagent adsorbed from the chemosynthesis of these polyols.

As can be seen from TG curve and more precisely from DTG curve of 5-OH polyol (Fig. 3a), the extrapolated onset temperature is 233.4°C and also presenting a less sharp DTG peak at 380°C in the second mass loss step from 324 to 512°C, due to the burnout of the residual carbonaceous material of the previous step.

The 10-OH polyol presents a different behavior during its first thermal decomposition step, which occurs from 150 to 316°C. The lower extrapolated onset temperature is 218.4°C and a distinctly lower DTG peak occurs at 265°C contrasting with the same decomposition step of the 5-OH polyol, because of its molecular structure in the polyol. However, the second decomposition mass loss step present a more homogeneous mass loss DTG peak than the other

**Table 2** TG results for three polyols under nitrogen atmosphere when $\beta$=10°C min$^{-1}$

| Project | 5-OH polyol | 10-OH polyol | 15-OH polyol |
|---|---|---|---|
| Onset *T*/°C | 233.4 | 218.4 | 186.8 |
| Primary region *T*/°C | 160–324 | 150–316 | 163–233 |
| Primary mass loss/% | 45.45 | 16.72 | 3.56 |
| Secondary region *T*/°C | 324–512 | 316–509 | 233–425 |
| Secondary mass loss/% | 41.83 | 82.24 | 83.59 |
| Tertiary region *T*/°C | – | – | 425–512 |
| Tertiary mass loss/% | – | – | 10.37 |
| Residue at 600°C/% | 0.56 | 0.39 | 0.94 |

polyols, as can be seen in the DTG curve (Fig. 3b). Its similar behavior to the other ones occurs because of the combustion of the carbonaceous residue.

The thermal decomposition of 15-OH polyol displays a different mass loss course showing three mass loss steps (Fig. 3c). The extrapolated onset temperature is 186.8°C and a sharpest DTG peak can be noticed at 378°C. The additional mass loss step occurs from 425 to 512°C and also presents a blurry DTG peak about 455°C. It is due to the introduction of nitrogen element into the 15-OH polyol caused the polyol has the function of higher thermal resistance. As a result the nitride from the second mass loss step decomposes in the last mass loss step.

It can be concluded that the onset temperature of the formal polyols decreases in the following order: 5-OH polyol >10-OH polyol >15-OH polyol in the first mass loss region.

The higher the onset temperature of decomposition of the polyol, the higher its thermal stability is. This property is of significant practical importance, especially when the polyols react with TDI, MDI, HDI and other type of diisocyanate to manufacture any useful polyurethane elastomer, in order to avoid the rupture of glyceryl chain of these formal polyols due to drastic exothermic reactions. The decomposition of the 5-OH polyol hydroxyl into water is difficult, but 10-OH polyols easier forms water from hydroxyl. 15-OH polyols are the most easily translated hydroxyl into water. It appears that the higher amounts of hydroxyl in the polyols can increase the thermal stability of these polyols and shift the process of mass loss toward higher temperatures. The hydroxyl in the 5-OH polyol can translate into carbon double bind (C=C) and 10-OH polyol can translate into a less stable three-membered ring (Scheme 2). The probability of the hydroxyl in the 10-OH polyol translating into a three-member ring is larger than for the 5-OH polyol once it has twice the number of hydroxyl. In the 15-OH polyol, the adjacent hydroxyl can easily translate into two different forms of more stable six-member rings (Scheme 2) during the first mass loss step. Consequently, the mass loss measured by TG shifted to somewhat higher temperatures in the secondary region of mass loss for these polyols. Taking the stability and probability of the ring being changed from the hydroxyl in different polyols into account, the thermal stability decreases in the following order: 15-OH polyol>10-OH polyol >5-OH polyol in the first mass loss steps.

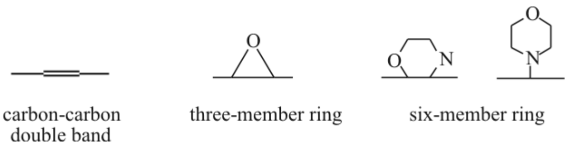

**Scheme 2** Part structure of the fatty acid carbon chains during degradation

*Kinetic analysis of polyols*

The kinetic study should be run above 150°C to ensure total vaporization of water from the atmosphere or reactants.

The kinetic decomposition of the polyols was analyzed with a non-isothermal technique. Friedman developed a differential isoconversional method whereby the activation energy for a mass loss process could be determined using Eq. (3) for the three formal polyols [14, 15]:

$$\lg\left(\frac{\beta \mathrm{d}\alpha}{\mathrm{d}T}\right)=\lg[AF(\alpha)]-\frac{E}{2.303RT} \tag{1}$$

and

$$\frac{\mathrm{d}x}{\mathrm{d}t}=\frac{\beta \mathrm{d}\alpha}{\mathrm{d}T} \tag{2}$$

then

$$\lg\left(\frac{\mathrm{d}x}{\mathrm{d}t}\right)=\lg[AF(\alpha)]-\frac{E}{2.303RT} \tag{3}$$

where $\beta$ is the heating rate, $T$ is the temperature, $t$ is the time, $R$ is the gas constant, $\alpha$ is the conversion degree, $A$ is the pre-exponential factor and $E$ is the activation energy in sense of Arrhenius equation. The slope of the straight line obtained by plotting $\lg(\mathrm{d}x/\mathrm{d}t)$ *vs.* $1/T$ at any level of same conversion degree can be used to calculate the activation energy for the mass loss process of formal polyols under nitrogen atmosphere. A typical $\lg(\mathrm{d}x/\mathrm{d}t)$ *vs.* $1/T$ plot calculated for the three formal polyols under nitrogen atmosphere is shown in Fig. 4.

The activation energy ($E$) of the polyol sample by the Friedman's analyses during the thermal degradation under nitrogen atmosphere is shown as Fig. 5. As can be seen from the thermal decomposition of 5-OH polyol, the activation energy is the lowest according to the appointed conversion degree in the three polyols. It shows that the 5-OH polyol has the lowest stability during thermal decomposition. A turning point is found to be at 332.2°C which is due to the three-member ring begins to rupture according to the 60% mass loss and then an approximate energy flat is come to appear with the reposeful decomposition.

The activation energy of 10-OH polyol slowly increases and ends at 316°C relating to 17.37% mass loss. The water from intramolecular reaction of adjacent hydroxyl of the10-OH polyol disappears and part fatty carbon chains partly rupture in the first mass loss step. The activation energy is 165 kJ mol$^{-1}$ is related

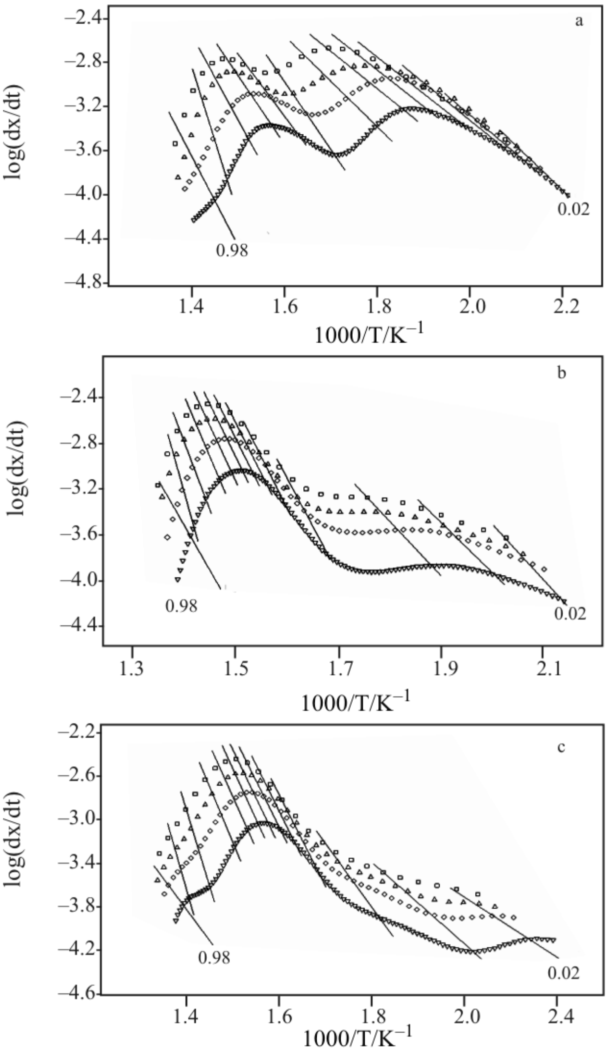

**Fig. 4** Friedman's analyses of: a – 5-OH polyol; b – 10-OH polyol; c – 15-OH polyol

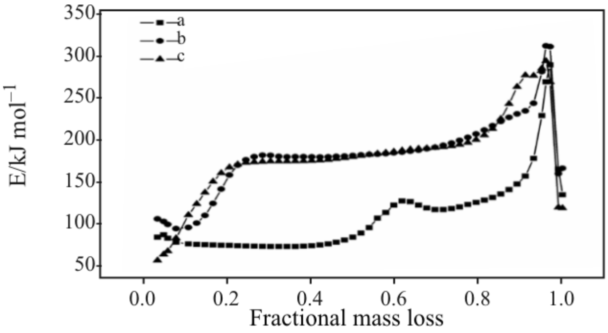

**Fig. 5** Activation energy plotted from Friedman's analyses: a – 5-OH polyol; b – 10-OH polyol; c – 15-OH polyol

to 19 mass% loss and is the beginning of three-member ring rupture. There is an energy plat ends at the temperature of 509°C till the three-member ring from the adjacent hydroxyl and fatty carbon chains decompose completely in the secondary mass loss.

The activation energy of degradation process of 15-OH polyol is similar to the 10-OH polyol, but the mass loss due to the disappearance of water from intramolecular reaction of adjacent hydroxyl is slightly prior to arrive because the six-member ring is more stable than three-member ring from 10-OH polyol. There is also a lesser turning point due to the appearance of the higher decomposition temperature of nitride.

## Conclusions

- Higher number-average functionality of hydroxyl in polyols cause the melting peaks to shift to higher temperatures and the shape of melting peaks to become smoother and wider, due to oligomerization.
- The thermal stability in an increasing order is: 5-OH polyol<10-OH polyol<15-OH polyol in the first mass loss steps because the extrapolated onset temperature of the polyols had the same order.
- The 5-OH polyol and 10-OH polyol had two mass loss steps but 15-OH polyol has an additional mass loss step because of the appearance of nitride at the higher decomposition temperature from the second mass loss step.
- The 15-OH polyol was prior to arrive at the mass loss region contrasted with the other samples because it had the highest stability and probability of the ring changed from the adjacent hydroxyl in the glyceride molecule.

## Acknowledgements

This paper is part of a project supported by Natural Science Foundation of Guangdong Province (No. 06025028).

## References

1 V. Logvinenko, V. Drebushchak, D. Pinakov and G. Chekhova, J. Therm. Anal. Cal., 90 (2007) 23.
2 S. Y. Jung and H. Yoshida, J. Therm. Anal. Cal., 89 (2007) 681.
3 M. Day, A. V. Nawaby and X. Liao, J. Therm. Anal. Cal., 86 (2006) 623.
4 E. Rudnik, G. Matuschek, N. Milanov and A. Kettrup, J. Therm. Anal. Cal., 85 (2006) 267.
5 L. Wachowski and M. Hofman, J. Therm. Anal. Cal., 83 (2006) 379.
6 C. C. Garcia, P. I. B. M. Franco, T. O. Zuppa, N. R. Antoniosi Filho and M. I. G. Leles, J. Therm. Anal. Cal., 87 (2007) 645.
7 J. Dweck and M. S. Sampaio, J. Therm. Anal. Cal., 75 (2004) 385.

8 J. C. O. Santos, I. M. G. Santos and M. M. Conceicao, S. L. Porto, M. F. S. Trindade, A. G. Souza, S. Prasad, V. J. Fernandes Jr. and A. S. Arauo, J. Therm. Anal. Cal., 75 (2004) 283.
9 J. Magoshi, M. A. Becker, Z. Han and S. Nakamura, J. Therm. Anal. Cal., 70 (2002) 833.
10 B. Kowalski, Thermochim. Acta, 184 (2001) 49.
11 A. Guo, Y. Cho and Z. S. Petrovic, J. Polym. Sci. A: Polym. Chem., 38 (2000) 3900.
12 A. Zlatanic, Z. S. Petrovic and K. Dusek, J. Biomacromol., 3 (2002) 1048.
13 G. L. Hasenhuette, Kirk, Othmer, Encyclopedia of Chemical Technology. R. E. Kirk, D. F. Othmer, J. I. Kroschwitz and M. Howe-Grant, Eds, Wiley, New York 1994.
14 H. L. Friedman, J. Polym. Sci., 6C (1965) 183.
15 T. Vlase, Gabriela Vlase and N. Doca, J. Therm. Anal. Cal., 80 (2005) 207.

Received: December 13, 2007
Accepted: May 28, 2008
OnlineFirst: August 15, 2008

DOI: 10.1007/s10973-007-8929-3